Articles
doi.org/10.1002/batt.202000324

Chemistry Europe
European Chemical Societies Publishing

Calendering of $Li(Ni_{0.33}Mn_{0.33}Co_{0.33})O_2$-Based Cathodes: Analyzing the Link Between Process Parameters and Electrode Properties by Advanced Statistics

Emiliano N. Primo,[a, b] Matthieu Touzin,[c] and Alejandro A. Franco*[a, b, d, e]

The optimization of the calendering process represents one of the key tasks for tuning the lithium-ion battery performance. In this study, we present a systematic statistical-based study of the three main calendering parameters (namely, the applied pressure, roll temperature, and line speed) effect on the porosity, electrode mechanical properties and electronic conductivity. Our work main goal is to understand how by changing the calendering parameters, the electrode properties can be tuned and up to which degree they determine the electrode capacity of $Li(Ni_{0.33}Mn_{0.33}Co_{0.33})O_2$-based cathodes. The statistical tools used for the analysis were the analysis of the covariance (ANCOVA), the principal components analysis (PCA), and the unsupervised machine learning k-means clustering algorithm. Our results showed that while porosity and the mechanical properties depend mainly on the applied pressure, the electrode's conductivity correlates mainly with the temperature. All of them were found to influence the cathode's capacity (at a rate equal to C), being the best condition applied pressures between 60 and 120 MPa and roll temperatures between 60 and 75 °C.

1. Introduction

The rise of electric vehicles/smart energy-grid storage have made research into lithium-ion battery (LIB) technologies increasingly significant.[1,2] Over the last decade, battery research has spanned a number of fields, from electrochemistry to nanotechnology.[3,4] This research has been mainly focused on the identification of superior active materials as a way to improve the power and energy performance of LIBs.[5] Nonetheless, the scientific community has recently acknowledged that the optimization of LIB manufacturing process is equally important if we aim to transition from a fossil fuel-based economy into an electric-based one.[6] The negative and positive electrodes are the key components of commercial LIBs, where discharging and charging electrochemical reactions take place. The electrodes are porous composites manufactured from particle-based laminates comprising a mixture of the active material with a conductive additive and a polymer binder. The manufacturing process consists therefore in the materials mixture into a liquid slurry, the coating over the current collector and evaporation of the dispersing solvent, the calendering and cutting, the electrolyte impregnation and the final battery cell assembly. Its electrochemical performance depends on an intricate relationship between the manufacturing process parameters and the physicochemical properties of the materials.[7–9]

Calendering is a critical step in the LIB production, as it reduces the electrode thickness by applying a compressive irreversible deformation at the surface of the electrode. In theory, the calendering process is well understood: the reduction in the electrode's porosity (ε) by compacting the laminate increases particle contact (therefore increasing the electronic conductivity) at the expense of increasing the electrolyte resistance within the porous electrode.[10] The optimum calendering condition is a trade-off between these two effects. In this sense, much of the work that has been done is focused on studying the impact of porosity reduction on the electrochemical performance/electrode microstructure,[11–13] on electronic/ionic conductivity,[14] or in the electrolyte wetting.[15,16] The question which is still open is how to tune those properties through controlling the calendering process parameters. Some hints to answer this have been recently studied and analyzed. In a recently published paper,[17] we developed an experimentally validated Discrete Element Method (DEM) model for simulating the calendering process of NMC-based cathodes, which explicitly considers the carbon-

[a] Dr. E. N. Primo, Prof. Dr. A. A. Franco
Laboratoire de Réactivité et Chimie des Solides (LRCS), UMR CNRS 7314
Université de Picardie Jules Verne, Hub de l'Energie
15 rue Baudelocque, 80039 Amiens Cedex 1, France
E-mail: alejandro.franco@u-picardie.fr
[b] Dr. E. N. Primo, Prof. Dr. A. A. Franco
Réseau sur le Stockage Electrochimique de l'Energie (RS2E),
FR CNRS 3459, Hub de l'Energie,
15 rue Baudelocque, 80039 Amiens Cedex 1, France
[c] Dr. M. Touzin
UMET - Unité Matériaux et Transformations
Univ. Lille, CNRS, INRAE, Centrale Lille, UMR 8207
59000 Lille, France
[d] Prof. Dr. A. A. Franco
ALISTORE-European Research Institute, FR CNRS 3104
Hub de l'Energie,
15 rue Baudelocque, 80039 Amiens Cedex 1, France
[e] Prof. Dr. A. A. Franco
Institut Universitaire de France
103 Boulevard Saint Michel, 75005 Paris, France

Supporting information for this article is available on the WWW under https://doi.org/10.1002/batt.202000324

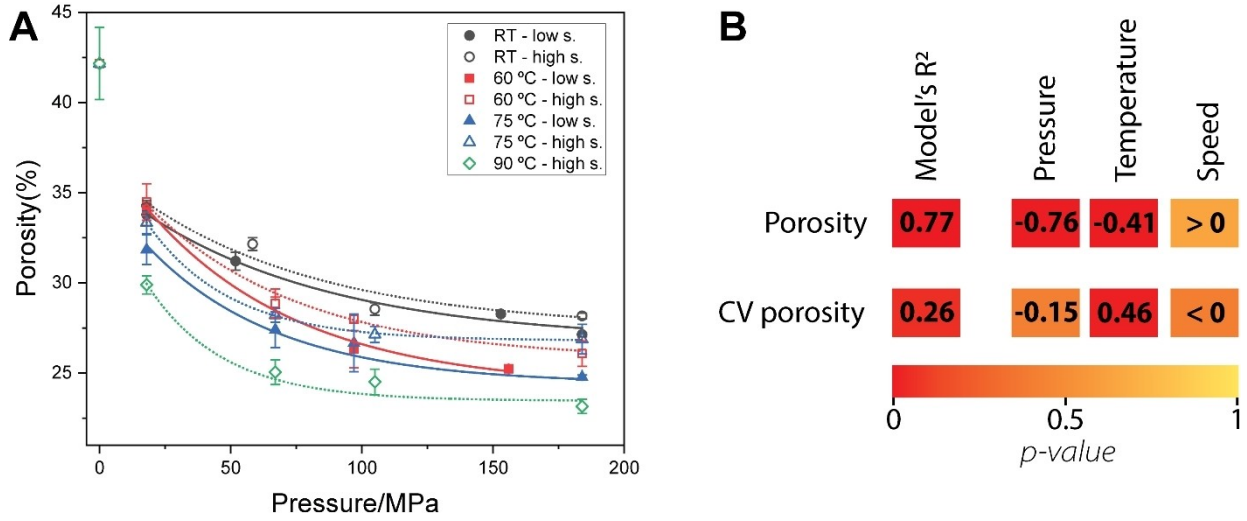

Figure 1. A) NMC cathodes porosity evolution when calendering at 25 °C (black circles), 60 °C (red squares), 75 °C (blue triangles) and 90 °C (green diamonds) at high (open symbols) and low (full symbols) speed. The lines correspond to the fitting of the data with the Heckel equation [Eq. (2)]. Table 1 shows the fitting output results. B) ANCOVA results for the porosity and its coefficient of variation (CV) in terms of the three calendering parameters. The numbers correspond to the Pearson's correlation coefficient between the observables and its explanatory variables while the color scale corresponds to the p-value.

binder domain and fully explains the impact of pressure on porosity, pore size distribution, tortuosity and electrochemical performance. The works from Schimidt *et al.*[18] and Lenze *et al.*[19] focused on developing empirical models for understanding the impact of calendering process parameters on the uncertainties and the key factors that condition the electrochemical performance upon reduction of the ε. Comprehensive research was also conducted to understand the impact of applied calender pressure, temperature and line speed (separately) over a range of properties such as pore size distribution, electrode mechanical features, coating density and rearrangement over different kind of electrodes, such as graphite, NMC and LMO.[20–23] Furthermore, we recently published a machine learning-experimental hybrid approach to rationalize the impact of calendering pressure over the ε, the electronic and ionic conductivities, particles contact with the current collector and active material active surface area for NMC-based cathodes in terms of the amount of active material used to prepare the electrodes.[10]

The quest towards the understanding and consequent optimization of the calendering process is still open and calls for more research in order to assess the electrode processability through this manufacturing step. In a previous work[24] we analyzed the impact of electrode formulation parameters (active material/carbon additive – binder relative ratio and amount of dispersing solvent) on the calendering processability and how that influences the electrode microstructure and electrochemical performance. In this work we aim to systematically study the three main calendering process parameters (namely applied calender pressure, roll temperature and line speed) over the electrode properties (such as porosity, mechanical properties and electronic conductivity) and how they determine the final capacity of NMC-based cathodes. Our study sheds light into which is the most relevant calendering parameter that controls each electrode property (and its homogeneity), supported by a statistics-based analysis of the experimental dataset. For that end, analysis of the covariance (ANCOVA), principal components analysis (PCA) and k-means clustering were used to understand the correlation and interdependencies between the observables (properties) and the explanatory variables (parameters). Furthermore, the optimum value of electrode capacity at high C-rate was linked to the set of parameters/properties which maximize it.

2. Results

Figure 1 displays the compaction curves (ε vs. calender pressure) for all the roll temperatures and line speeds. As in our previous work,[24] the fitting with the modified Heckel equation including the un-calendered electrode was not possible due the abrupt decrease in ε at low pressures. Table 1 presents the fitted minimal attainable porosities (ε_{min}) and compaction resistances (γ_C) extracted from the Eq. (2). In terms of the temperature, both ε_{min} and γ_C are smaller as it increases. Being the PVdF a thermoplastic polymer,[25] the increase in the temperature facilitates the polymer deformability and therefore lower porosities can be reached.

Table 1. Compressibility factor (γ_C) and minimal attainable porosity (ε_{min}) derived from the Heckel equation fitting of the data in Figure 1.

Condition	γ_C/MPa	ε_{min}
RT-low speed	73 ± 2	27.1 ± 0.1
RT-high speed	70 ± 3	28.2 ± 0.2
60 °C-low speed	58 ± 3	25.2 ± 0.2
60 °C-high speed	57 ± 4	26.1 ± 0.7
75 °C-low speed	49 ± 2	25.6 ± 0.1
75 °C-high speed	41 ± 2	25.8 ± 0.8
90 °C-high speed	28 ± 3	23.1 ± 0.4

The ε ANCOVA analysis shows that 77% of its variability is explained by the calendering parameters, with a good model confidence (p-value <0.0001). In terms of the calendering parameters, both pressure and temperature explain the ε variance while the line speed does not have a statistically relevant effect (p-value $=0.6465$). Between the applied pressure and the temperature, the first parameter is more correlated to the ε. Naturally, the negative sign of both coefficients indicates that by increasing the applied pressure/temperature, ε is reduced. Another important parameter is the coefficient of variation (CV), which is defined as the ratio of the standard deviation to the mean. The CV gives information about the dispersion, repeatability and reproducibility of a property. The ANCOVA shows that only 26% of the ε CV variability is explained by the pressure, temperature and speed and, quite interestingly, there is a positive correlation with the temperature ($R^2>0$). This means that the ε dispersion decreases with increasing roll temperatures. Nonetheless, such a low R^2 for the ANCOVA suggests that the conclusions should be taken with caution and more explanatory variables should be taken into account.

Through the microindentation measurements, the electrodes mechanical properties were obtained. The hardness (H) represents the resistance to plastic deformation and is a very important feature as it is inversely related to the ε and ε_{min}.[24] Figure 2A displays the H in terms of the applied calender pressure for the four different roll temperatures and two line speeds, while Figure 2C presents the results of the ANCOVA test. Increasing the temperature and the pressure produces an increase in the electrodes H ($R^2>0$), as expected. The ANCOVA analysis shows that both parameters are equally correlated with H while the line speed (having a p-value equal to 0.993) does not bring any significant changes into H variability. In terms of H CV, its variance is explained by the pressure and temperature: when increasing both parameters, the CV increases; being the pressure the variable more strongly correlated (higher R^2).

Another relevant mechanical property is the ratio W_{el}/W_{pl}, which is related to the contact strength between the polymer (PVdF) and the solid particles (NMC, CB)/current collector and allows to infer in the electrode adhesion.[26] The changes in W_{el}/W_{pl} as a function of the calendering parameters, displayed in Figure 2B, do not show any apparent trend. Furthermore, the explanatory variables (Figure 2D) are responsible of only 29% of W_{el}/W_{pl} variability, indicating a low correlation. Nonetheless, the profiles show that at low-medium pressures there seems to be a trend that is completely lost at high pressures and high temperatures. By performing a k-means clustering analysis on

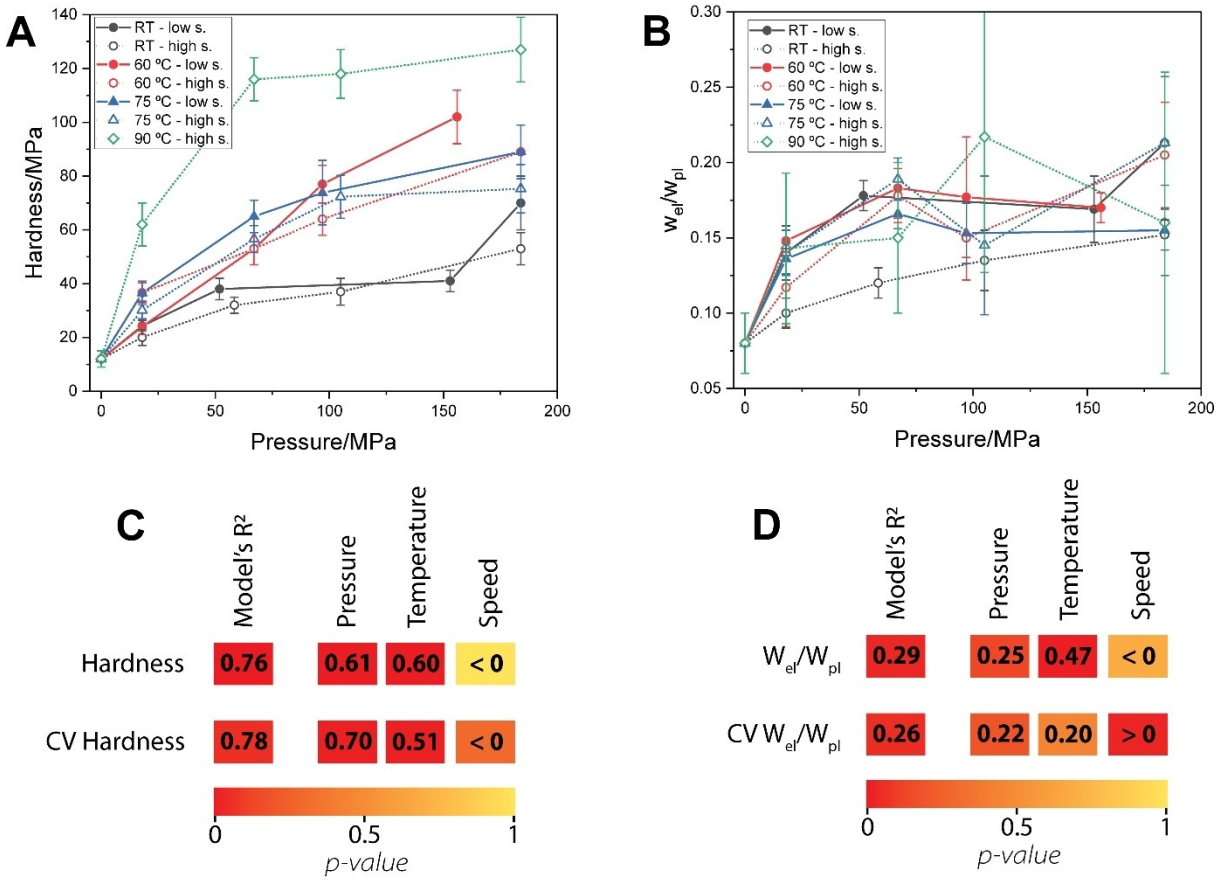

Figure 2. Average hardness (A) and elastic-to-plastic work ratio (B) in terms of the calendering parameters. ANCOVA results for the hardness and its CV (C) and the W_{el}/W_{pl} ratio and its CV (D) in terms of the calendering parameters. The numbers correspond to the Pearson's correlation coefficient between the observables and its explanatory variables while the color scale corresponds to the p-value.

W_{el}/W_{pl} in terms of the calender pressure, temperature and speed, 2 distinct groups can be found (section 2 in the Supporting Information). The first one corresponds to low-medium pressures and the second one, to high pressures. An ANCOVA test over the first one shows that both pressure and temperature are directly correlated with W_{el}/W_{pl} (R^2 equal to 0.69 and 0.50, respectively) while speed does not have a significant impact (p-value = 0.882). For the second group (high pressure), the explanatory variables do not bring significant information into W_{el}/W_{pl} variability (model's p-value = 0.28). This suggests that the electrode adhesion can be increased through calendering up to a certain point. Furthermore, high pressures/high calendering temperatures output higher CV for the adhesion properties (Table S1 in the Supporting Information). This is also consistent with the previous conclusion: if the electrode adhesion can be increased up to certain calendaring conditions, above it we will favor inhomogeneities in the particle distribution/electrode current collector contact points.

The electronic conductivity plays a significant role in the performance of LIB as it accounts for the electron transport through the porous electrode[27] and can become the limiting factor for high-power applications.[28,29] As the electrode is an anisotropic composite, its conductivity depends on the connectivity between the particles and, therefore, can be tuned through the calendering process.[10] Figures 3A and B present the NMC cathodes K_{dry} dependence upon the calendering parameters and its corresponding ANCOVA test output. From the profiles it can be seen a non-monotonic profile in terms of the three calendering parameters and, in consequence, they account for 44% of K_{dry} variability. Furthermore, temperature is mainly correlated to K_{dry}. A qualitative analysis of the profiles unveils 3 features: (i) K_{dry} has a maximum at intermediate pressure, (ii) up to 75 °C, the changes in K_{dry} are small in terms of the roll temperature and line speed, and (iii) at 90 °C (and even at high line speed) there is an important increase in K_{dry}. This behavior is linked with the major changes in both ε and H when calendering at 90 °C, indicating a significant increase in the electrode's compaction.

During the electrolyte impregnation stage, the electrodes experience some mechanical deformation due to the polymer network solvent uptake and its consequent swelling.[30] This is reflected in a conductivity decrease after the electrolyte imbibition (K_{soaked}), regardless of the calendering condition, as depicted in Figure 3C. In this case a monotonic increase in K_{soaked} can be seen for temperatures up to 60 °C while for 75 °C low speed and 90 °C high speed a maximum-type behavior at intermediate pressures can be seen. This is consistent with the W_{el}/W_{pl} results, as particle contact can be increased up to a certain point, above which major changes in the electrode microstructure favor a particle contact loss and consequently, a less effective percolating network. The ANCOVA analysis shows that the roll temperature is the calendering parameter that explains the most variability. As PVdF deformability increases with temperature, higher roll temperatures favor the polymer rearrangement in a way that minimizes the polymer swelling. This can also be seen in the changes of the K_{soaked}/K_{dry} ratios (Figure 3E and F). As the conductivity gets reduced upon wetting, all the ratios are lower than one and, amongst all the calendering conditions, 75 and 90 °C roll temperatures exhibit the highest K_{soaked}/K_{dry}. The ANCOVA analysis attest a 62% of its variability described by the explanatory variables, mainly from temperature.

The electronic conductivity being mainly dictated by temperature means that a rearrangement of the polymer layer is required for increasing the number of contacts in the percolating network. This is supported by the fact that higher calendering temperatures correspond to higher K_{soaked}/K_{dry} ratios and, consequently, to less swelling upon wetting with the electrolyte. Furthermore, this feature is not due to a simple effect of ε reduction: when comparing different pressure and temperature calendering conditions with the same ε (Figure S2, in the Supporting Information), the electronic conductivities are different. In this sense, high temperatures favor the densification of the CB/PVdF phase, with higher number of contact points.[31]

3. Discussion and Impact Over the Cathode's Capacity

The PCA output allows to analyze at a glance all the observables and their interdependencies (section 4, in the Supporting Information). The first two principal components account for 84% of the observable's variance (PC1 = 70.9 and PC2 = 13.1%). The squared cosines table (Table S2 in the Supporting Information) shows that all the electrode properties are mainly correlated to PC1 and PC2, so there is no need to consider further ones. The orange vectors in Figure 4A represent the electrode properties projections on the new dimensions found by the PCA: ε is inversely correlated with the H, K_{dry}, K_{soaked} and its ratio. From all of them, H is the one that is more correlated, meaning that the ε controls naturally the compactness of the electrode. Furthermore, K_{dry} and K_{soaked} (and their ratio) are inversely related with the ε. These results agree with the correlations already found with the calendering parameters. In the case of W_{el}/W_{pl}, its projection is almost orthogonal to all the other properties, meaning low correlation. The squared cosines table (Table S2) shows that PC2 is strongly linked only with W_{el}/W_{pl}, while the others are associated with PC1. Although the correlation matrix (Table S1 in the Supporting Information) also exhibits low correlation with the other variables ($R^2 < 0.5$), it can be seen that W_{el}/W_{pl} increases with the conductivities and the H and with decreasing ε. As this property is related with the contacts between the particles and the binder adhesion, its low sensitivity in terms of the calendering conditions can be related to the low amount of polymer and carbon additive used for the electrode formulation. Besides us, few studies have dealt with the calendering impact on the electrode adhesion.[23,32] Non-linear relations were also found on those studies and it was also concluded that the loss of particle contact sensitivity towards calendering when working with low binder/carbon additive electrodes. It is worth mentioning that adding further PC axes, and therefore

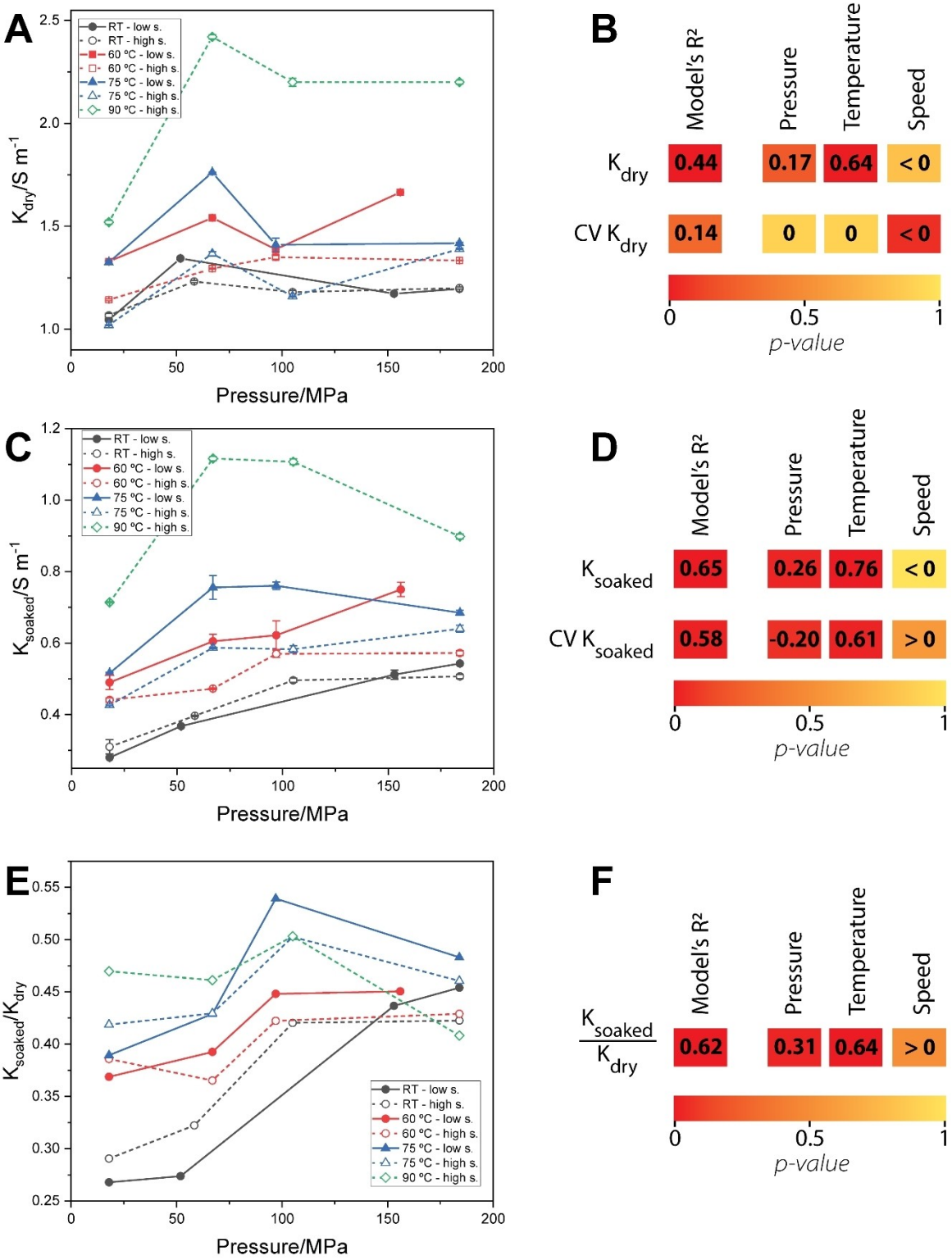

Figure 3. Dry electrode electronic conductivity (K_{dry}) in terms of the calendering parameters (A) and the ANCOVA test output (B). Soaked electrode electronic conductivity (K_{soaked}) in terms of the calendering parameters (C) and the ANCOVA test output (D). K_{soaked} to K_{dry} ratio in terms of the calendering parameters (E) and the ANCOVA test output (F).

considering higher variability, would not increase the representation quality (low squared cosine values for PC3 and PC4).

The dots in Figure 4A represent the observations in the PC1-PC2 space, whose properties can be easily inferred by their positions relative to the projection vectors. A k-means clustering run over the observations in the PCA space (Figure S4, in the Supporting Information) gave five different groups, which can be seen in different colors in Figure 4A. In order to

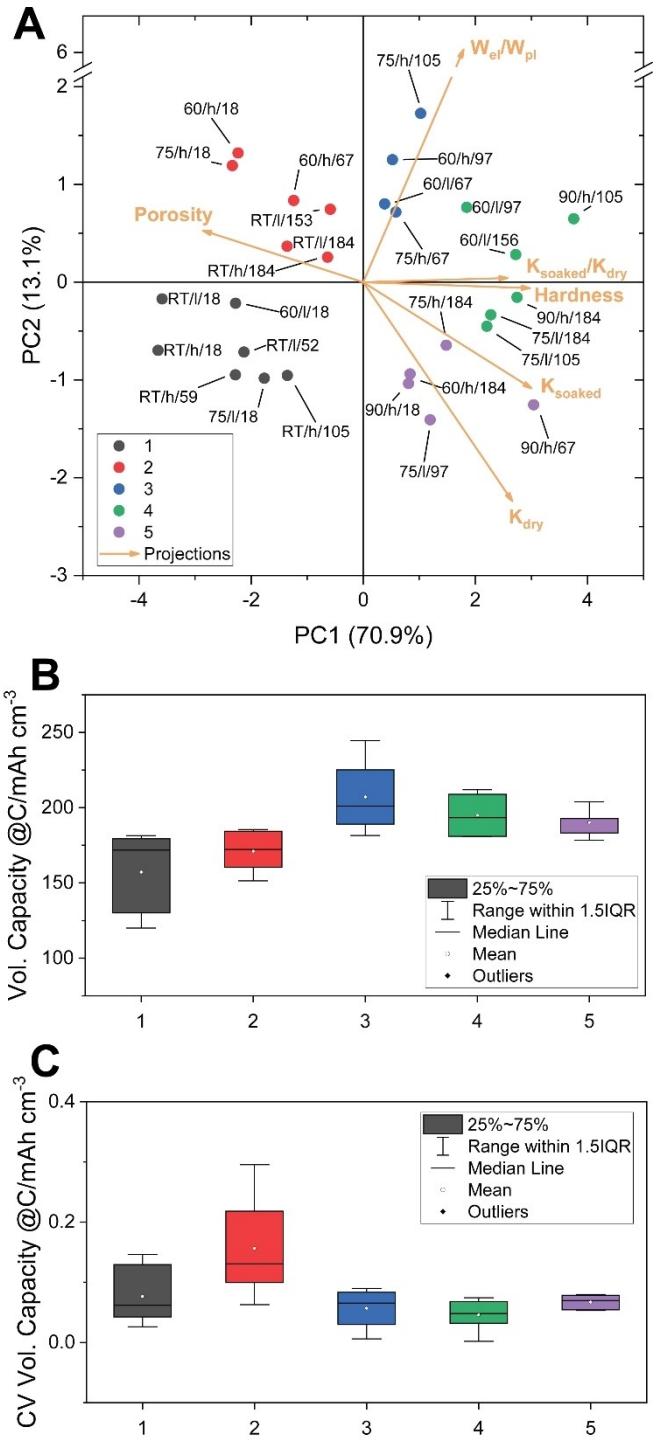

Figure 4. A) PCA output of the correlations between the electrode porosity, mechanical properties and electronic conductivity. The orange vectors correspond to the variables' projections over the two first principal components (PC1 and PC2). The dots correspond to the 28 different calendering conditions plotted in the PC1-PC2 space. The labels correspond to the calendering conditions of each one (temperature/speed [h or s]/pressure) while the colors represent the different classes given by the k-means clustering analysis. B and C) Volumetric capacities and its coefficient of variability (CV) box plots, grouped by the k-means clustering analysis output.

understand the effect of calendering over the cathode electrochemical performance, the capacity for each cluster is depicted in the Box plots of Figure 4B. We normalized the capacity by the electrode volume in order to take into account the effect of thickness reduction upon calendering, which impacts positively the energy and power density.[29] In this sense, the electrode compaction is one of the most straightforward ways to increase a battery nominal capacity/power. There are 2 distinctive groups, with lower ($k=1$ and 2) and higher ($k=3$, 4 and 5) normalized capacity values, which are statistically different between them (determined through a Kruskal-Wallis test with $\alpha=0.05$). The classes with the highest capacities correspond to the electrodes calendared at temperatures equal to 60 °C (intermediate to high pressures), 75 °C (intermediate to high pressures) and 90 °C (all pressures), irrespective of the line speed. For the case of the normalized capacity CV, the lowest values correspond to $k=3$, 4 and 5 (Figure 4C). Figure S5, in the Supporting Information, displays the Box plots for each cluster according to the six electrode properties. The groups with the highest capacity/lowest CV correspond to the ones with $\varepsilon<$ 27 %, mid-to-high H and K_{soaked} and K_{soaked}/K_{dry} ratios. In the case of W_{el}/W_{pl}, for $k=3$ there is a significant difference relative to the other groups which is interestingly the class with the highest capacity. Furthermore, this group is the one that has intermediate values for all the other properties.

Figure 5A shows the main correlations of all the electrode properties in terms of the applied pressure and temperature, coming from the ANCOVA tests. This graph gives at a glance the main controlling parameters over each electrode property, by checking to which axis that property is closer to. Note that line speed was not considered, as in all the ANCOVA tests performed no significant impact on the observables' variabilities was found. This is probably due to low line speed operating interval (which is constrained by the calendering machine) and it is expected that at higher line speeds this parameter should have some effect.[33] Porosity is mainly controlled by the calendering pressure (negative correlation) while the mechanical properties have a shared temperature/pressure control (positive correlation). For the case of the particle contact strength/electrode adhesion (W_{el}/W_{pl}), a very low percentage of its variability is explained by the calendering parameters, as discussed before. Although it is generally assumed that upon increasing the electrode compactness the adhesion strength increases, our results reveal that a systematic measurement of this property should be always performed (according to the specific electrode formulation/calendering conditions) and not assumed.

The ε/mechanical properties inhomogeneities have a direct correlation mainly with pressure. Therefore, when optimizing the manufacturing procedure, special care must be taken when calendering as if high applied pressures are needed, then we would risk to increase the electrode properties deviations. This is known to have a huge impact on battery durability and rejection rate.[7,34,35] The electrode conductivity is mainly controlled by the temperature, indicating that for having a good conductive particle inter-connectivity (percolation) we must rely on PVdF thermoplasticity. In terms of electrode formulation, it is known that the electronic conductivity sensitivity towards the calendering parameters is lower when higher

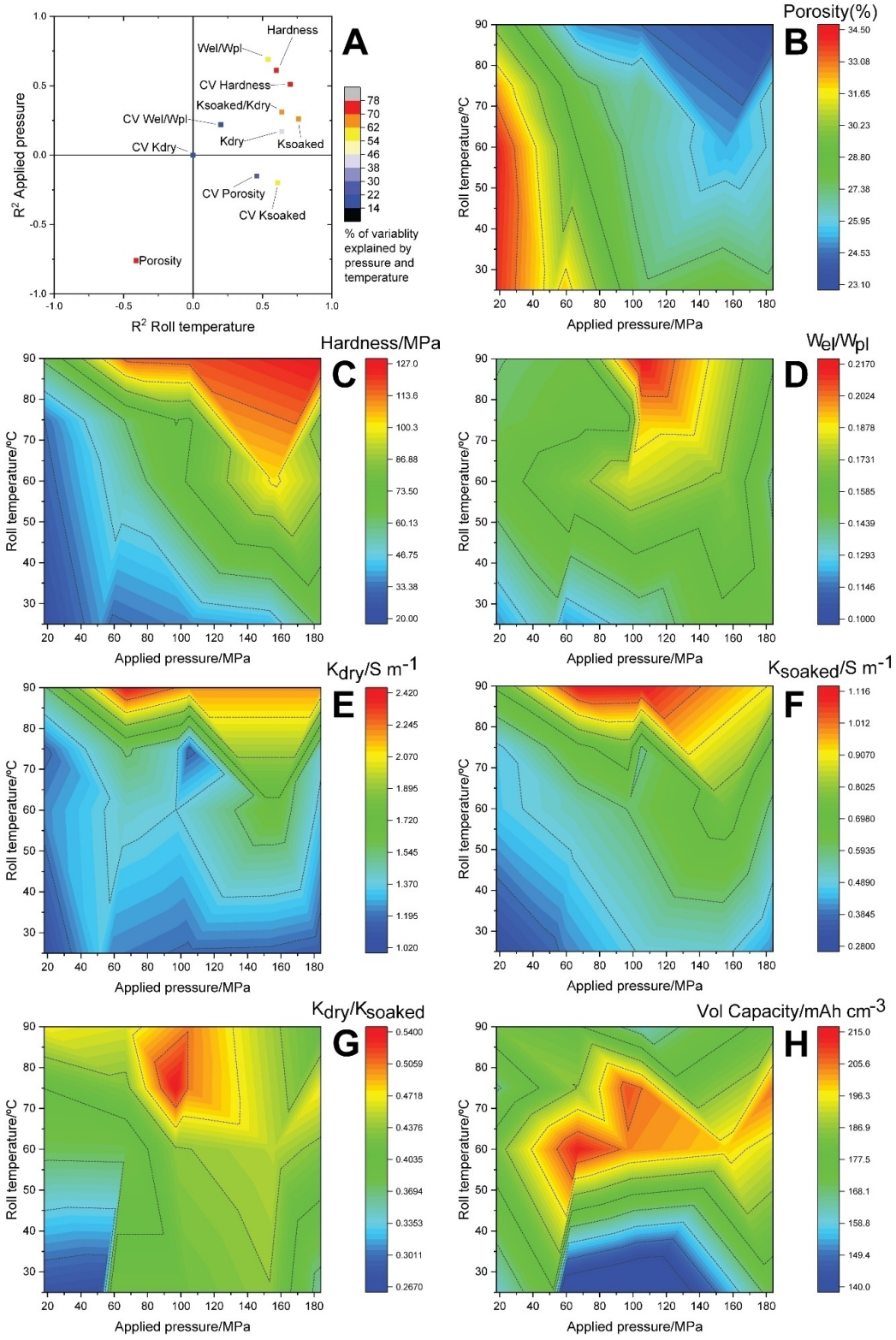

Figure 5. A) Correlation coefficients plot (applied pressure vs. temperature) derived from the ANCOVA analysis of each electrode property. The color bar represents the percentage of variability of each property explained by the calendering parameters pressure and temperature. B–F) 2D heat-maps of each electrode property in terms of the applied calender pressure and roll temperature.

amounts of CB/PVdF are used.[31] Nonetheless, high PVdF-content electrodes are expected to undergo major rearrangement upon increasing the calendering temperature. Further investigations are being carried out by our group in order to understand the changes in conductivity in terms of the electrode formulation parameters. Most important, and rarely

acknowledged, the electrolyte wetting induces a decrease in K and its dependency can be explained by the calendering parameters. Furthermore, higher temperature favors a lower decrease in the electronic conductivity at the expense of higher deviations in K_{soaked}.

Being the cathode's capacity a trade-off of several electrode properties, their highest values were found at intermediate temperatures (60–75 °C) and applied pressure (60–120 MPa), as it can be seen on panel H of Figure 5. The same region in the other electrode properties heat-maps is associated to intermediate values of ε, H and W_{el}/W_{pl}. Furthermore, the comparison of K_{dry} and K_{soaked} (Figure 5 E and F) shows that is mainly the latter which explains the percolation network of the electrode. It is known that upon decreasing the ε, the electrolyte effective conductivity decreases,[10,36] which negatively impacts the electrochemical performance. Higher temperatures combined with higher applied pressure induce a drastic reduction of pore volume fraction and electrode compactness that although is beneficial for the electrode conductivity, it outputs a major increase in the electrode's tortuosity.

4. Conclusions

In this work we systematically studied the impact of the calendering parameters over the porosity, electrode mechanical properties, electronic conductivity and its link with the electrochemical performance. 28 different conditions were analyzed through advanced statistics tests to understand the correlation and main controlling parameters. It was found that while both temperature and pressure reduce the porosity, the main influencing parameter is the latter. In terms of the mechanical properties, there is a direct correlation between the porosity reduction and the increase in the electrode compactness (hardness) while in terms of the adhesion the dependence is weaker, probably due to the low amounts of PVdF and carbon additive used. We further demonstrated that electronic conductivity increase depends mainly on the calendering temperature and that the latter is better correlated when measuring after the electrolyte impregnation, due to the polymer swelling at this stage. Naturally, it was found that the calendering impacts the volumetric capacity of the NMC-based cathodes. It is maximized at intermediate applied pressures (60–120 MPa) and intermediate temperature (60–75 °C). These conditions are related to intermediate values of all the measured electrode properties. Naturally, the optimum calendering conditions are machine-dependent and, therefore, they will probably change when using another calendering system. Nonetheless, the analysis methodology performed throughout this work not only remain valid but also provide guidelines to precisely control the calendering parameters in order to tune the electrode properties. It also presents a consistent and systematic statistics/machine learning-based analysis approach to be applied to other manufacturing steps.

Experimental Section

$LiNi_{1/3}Mn_{1/3}Co_{1/3}O_2$ (NMC, average particle diameter = 5 ± 3 μm) was supplied by Umicore. C-NERGY™ super C65 carbon black (CB) was supplied by IMERYS. Solef™ 5130/1001 Polyvinylidene fluoride (PVdF) was purchased from Solvay and *N*-methylpyrrolidone (NMP) from BASF. All the other reagents were battery grade and were used without further purification.

Electrodes Processing

The slurry solid components NMC, CB and PVdF (96:2:2, in wt%) were premixed with a soft blender. Afterwards, NMP was added until reaching a ratio between the solid components and the solvent equal to 0.69. The mixture was performed in a Dispermat CV3-PLUS high-shear mixer for 2 h in a water-bath cooled recipient at 25 °C. The slurry was coated over a 22 μm thick Aluminum current collector using a comma-coater prototype-grade machine (PDL250, People & Technology, Korea), fixing the gap at 300 μm and the coating speed at 0.3 m min^{-1}. The electrodes were dried in a built-in two-parts oven at 80 and 95 °C. The mass fraction and thickness of the electrodes were 39.5 ± 0.8 mg cm^{-2} and 180 ± 4 μm respectively.

The electrodes (dimension = 10 × 20 cm^2) were calendered with a prototype-grade lap press calender (BPN250, People & Technology, Korea). The latter consists in a two-roll compactor of 25 cm of diameter in which the gap between the rolls controls the pressure applied to the electrodes. The calendering was performed at various applied pressures, in terms of the line speed (0.54 and 1.82 m min^{-1}) and four different roll temperatures (25, 60, 75 and 90 °C). The applied calender pressure was obtained by measuring the applied force of the corresponding roll gap through the utilization of a force sensor film (ELF measuring system equipped with FlexiForce sensors, Tekscan) and then normalizing by the contact area between the electrode and the roll.

Electrodes Characterization

Porosities were calculated according to Equation (1):

$$\varepsilon = 1 - \frac{m_{el}\,(X_{NMC}/\rho_{NMC} + X_{CB}/\rho_{CB} + X_{PVdF}/\rho_{PVdF})}{V_{el}} \quad (1)$$

where X and ρ are the mass fractions in the electrode and densities of the three solid components NMC/Carbon Black (CB)/PVdF and m_{el} and V_{el} correspond to the electrode mass and volume, respectively. The porosities were measured on 10 different 13 mm-diameter disks (punched from different regions of the calendered film electrodes) so the results presented in this work represent an average with $n = 10$.

The analysis of ε vs. calender pressure profiles is based on the Heckel equation[37] [Eq. (2)], which was adapted to analyze the compressibility of composite electrodes,[23] as shown in Eq. (2):

$$\varepsilon = \varepsilon_{min} + (\varepsilon_0 - \varepsilon_{min})\,\exp\left(\frac{-P}{\gamma_C}\right) \quad (2)$$

where ε_0 and ε_{min} are the initial and minimum attainable porosities, respectively, P is the calender applied pressure and γ_C is compaction resistance.

Microindentation experiments were carried out at room temperature with a microhardness Tester (MHT, CSM Instruments)

equipped with a Vickers diamond indenter. The loading/unloading rate was 0.4 mN s^{-1} and the maximum load for all the indentation experiments was of 200 mN, which ensures an indenter penetration lower than 10% of the electrodes thickness, in order to avoid substrate effects. Before unloading, the indenter was maintained at the maximum load during 3 s. Thirty indentation tests were performed for each testing condition to ensure representative results. The electrodes hardness (H) was determined by the Oliver-Pharr method.[38] The ratio between the elastic and plastic work (W_{el}/W_{pl}) was obtained from each indentation curve by integrating the area beneath the loading ($W_{pl}+W_{el}$) and unloading (W_{el}) curves. The difference between the areas of the loading and unloading curves is equal to W_{pl}.

Electrochemical characterizations were performed in 2032-type coin cells in a half-cell configuration (working electrode area: 1.327 cm^2) with a Li foil counter/reference electrode. A 1.0 M $LiPF_6$ solution in ethylene carbonate:dimethyl carbonate (1:1 wt.) was used as the electrolyte. The half-cells were assembled in a glovebox (Braun) with a H_2O and O_2 content lower that 0.1 ppm. The galvanostatic charge/discharge experiments were carried out using a BCS-810 series battery cycler (BioLogic, Seyssinet-Pariset, France) in the voltage range of 3.0–4.3 V. The formation cycle was performed by cycling the cell in the same voltage range at C/10. The half-cells were cycled at C/10, C/5, C and 2 C and then back to C/10 for 5 charge/discharge cycles each, except for the last C/10 which was done for 10 cycles. The capacities reported in this work correspond to the average value at a rate equal to C, normalized by the electrode volume. This is because at high current regime the kinetic limiting factors are the ones that determine the electrochemical response.[39] 1 C corresponds to the current for discharging an NMC electrode in 1 hour (specific capacity = 170 mAh g^{-1}). Reported electrochemical results correspond to the average of 5 different independent experiments. All the electrochemical experiments were performed at 25 ± 1 °C.

Electrical conductivities were measured in two different conditions, pristine dry and after wetting with the electrolyte. To that end the aluminum current collector was carefully peeled off from the electrode film. The first one (K_{dry}) was performed by obtaining the electronic resistance (R) through electrochemical impedance spectroscopy (EIS). A MTZ-35 frequency response analyzer and an intermediate temperature system (BioLogic, Seyssinet-Pariset, France) were used to perform the EIS analysis. The peeled off electrode (2×1 cm^2) was introduced into a controlled environment sample holder (CESH) to perform AC impedance measurements under air at 25 °C using an in plane 4-points gold electrode. A frequency range of 1 MHz to 1 Hz (20 points per decade and 10 measures per points) and an amplitude voltage of 0.05 V were applied during the measurements. The electrical conductivity of the electrode soaked with the 1 M $LiPF_6$ electrolyte (K_{soaked}) was measured through DC polarization, by applying voltages of 0.10, 0.15 and 0.20 V for 15 min to determine the electronic resistance. After the application of the potential perturbation (E_{DC}), the current decays to its steady-state value ($i_{s\text{-}s}$) and R is calculated through Ohm's law as $E_{DC}/i_{s\text{-}s}$. Both conductivities were obtained through Eq. (3):

$$K = \frac{\ell}{A\,R} \tag{3}$$

where ℓ is 1 cm and the area A is calculated as the product of 1 cm and the electrode thickness.

Statistical Analysis Methodology

All the electrode properties (porosity, mechanical properties, electronic conductivity and electrochemical performance), tabulated in terms of the calendering process parameters (applied calender, pressure, roll temperature and line speed), are shown in the Supporting Information (section 1). To quantitatively understand the impact of the parameters on the properties, an analysis of the covariance (ANCOVA) was performed (Figure 6A). The ANCOVA is used to test the main interaction effects of independent categorical variables on a continuous dependent variable, controlling in the meantime the impact of selected other continuous variables, which are called the covariates. This statistical test is a combination of ANOVA with linear regressions and is very useful to remove the effects of variables which modify the relationship of the categorical independents to the dependent interval. In our case, the ANCOVA was used to independently assess the effect of the applied calender pressure, the roll temperature (both quantitative) and the line speed (considered here as qualitative) on the selected electrode property. In terms of the explanatory variables, both the Pearson's correlation coefficients (R^2) and the type III sum of squares p-value were used to assess their impact on the observables. The magnitude of R^2 gives insight into the correlation strength while its sign (positive/negative) represents if there is a direct or indirect correlation, respectively, i.e. if by increasing the parameter value, the property gets increased or reduced. The goodness of the fit was evaluated by the model's R^2, where the effect of the explanatory variable was determined by testing the equality of mean values between each group, according to the p-value test. The p-value corresponds to the risk in rejecting the null hypothesis (no significant differences) with $\alpha = 0.05$ and it spans between 0 and 1. The closer the p-value is to 0, the higher the validity of assuming that the model and/or the explanatory variables explain the observable's variance. Before performing each ANCOVA, the validity of its assumptions was evaluated by performing Shapiro-Wilk (normality of the residuals) and Levene's (homoscedasticity) test on the explanatory variables.

For the data visualization/classification in a multivariate space two statistical methods were implemented: principal component analysis (PCA) and k-means clustering (Figure 6B). PCA is a features extraction method for low-dimensional space reduction as it projects observations from a p-dimensional space with p variables to a m-dimensional space (where $m < p$) so as to conserve the maximum amount of information (*i.e.* the total variance of the dataset) from the initial dimensions. The new m variables are a linear combination of the original p and are called principal components (PC). k-means clustering is a very powerful unsupervised machine learning algorithm which sorts similar items in k clusters (characterized by the cluster centroid), without any prior information on labeling of the dataset. It normally works by defining randomly the centroid position of the k clusters and classifying each point to the nearest centroid. The algorithm will then minimize within-cluster variances (Sum of Square Error, SSE) in each step until reaching a certain tolerance value. The choice of the optimum k is generally done manually, by launching several k-means clustering with different k values, selecting the one that does not improve any further the SSE. All the statistical tests were implemented through the XLSTAT add-on for Excel.

Acknowledgements

A.A.F. and E.P. acknowledge the European Union's Horizon 2020 research and innovation programme for the funding support through the European Research Council (grant agreement

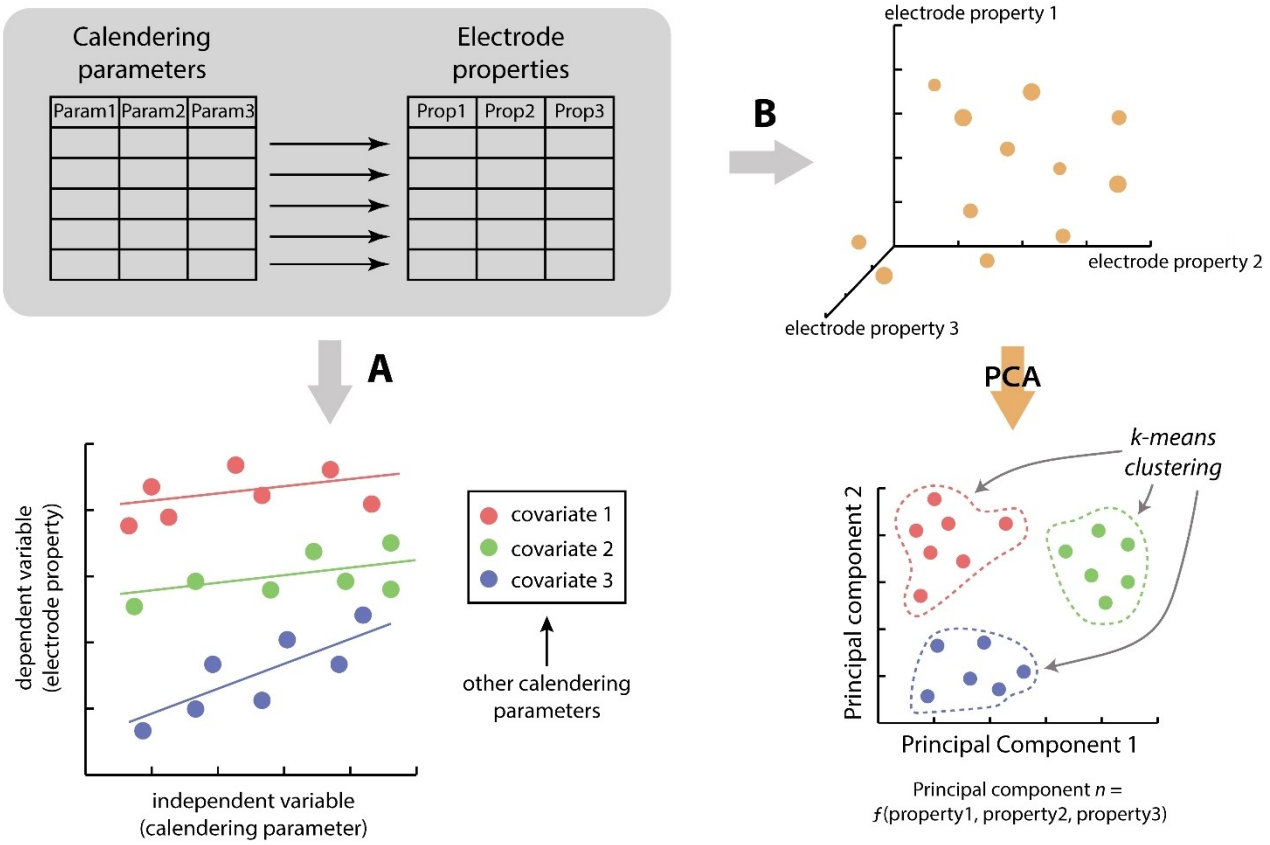

Figure 6. Statistical methodology followed for the analysis of the calendering parameters/electrode properties dataset in this work.

772873, "ARTISTIC" project). A.A.F. acknowledges Institut Universitaire de France for the support. The authors acknowledge Marc Duquesnoy (LRCS) for useful discussions on statistical methods.

Conflict of Interest

The authors declare no conflict of interest.

Keywords: NMC cathodes · calendaring · statistical analysis · mechanical properties · electrochemical performance

[1] W. Xie, X. Liu, R. He, Y. Li, X. Gao, X. Li, Z. Peng, S. Feng, X. Feng, S. Yang, *J. Energy Storage* **2020**, *32*, 101837.
[2] J. I. Chowdhury, N. Balta-Ozkan, P. Goglio, Y. Hu, L. Varga, L. McCabe, *Renewable Sustainable Energy Rev.* **2020**, *131*, 110018.
[3] L. Yu, X. Zhou, L. Lu, X. Wu, F. Wang, *ChemSusChem* **2020**, *13*, 5361.
[4] S. Maddukuri, D. Malka, M. S. Chae, Y. Elias, S. Luski, D. Aurbach, *Electrochim. Acta* **2020**, *354*, 136771.
[5] L. Wen, J. Liang, J. Chen, Z.-Y. Chu, H.-M. Cheng, F. Li, *Small Methods* **2019**, *3*, 1900323.
[6] A. Kwade, W. Haselrieder, R. Leithoff, A. Modlinger, F. Dietrich, K. Droeder, *Nat. Energy* **2018**, *3*, 290.
[7] M. Thomitzek, O. Schmidt, F. Röder, U. Krewer, C. Herrmann, S. Thiede, *Procedia CIRP* **2018**, *72*, 346.
[8] S. Thiede, A. Turetskyy, A. Kwade, S. Kara, C. Herrmann, *CIRP Ann.* **2019**, *68*, 463.
[9] S.-H. Park, R. Tian, J. Coelho, V. Nicolosi, J. N. Coleman, *Adv. Energy Mater.* **2019**, *9*, 1901359.
[10] M. Duquesnoy, T. Lombardo, M. Chouchane, E. N. Primo, A. A. Franco, *J. Power Sources* **2020**, *480*, 229103.
[11] X. Lu, A. Bertei, D. P. Finegan, C. Tan, S. R. Daemi, J. S. Weaving, K. B. O. Regan, T. M. M. Heenan, G. Hinds, E. Kendrick, D. J. L. Brett, P. R. Shearing, *Nat. Commun.* **2020**, *11*, 1.
[12] X. Lu, S. R. Daemi, A. Bertei, M. D. R. Kok, K. B. O'Regan, L. Rasha, J. Park, G. Hinds, E. Kendrick, D. J. L. Brett, P. R. Shearing, *Joule* **2020**.
[13] D. Schmidt, M. Kamlah, V. Knoblauch, *J. Energy Storage* **2018**, *17*, 213.
[14] V. Laue, F. Röder, U. Krewer, *Electrochim. Acta* **2019**, *314*, 20.
[15] A. Davoodabadi, J. Li, H. Zhou, D. L. Wood, T. J. Singler, C. Jin, *J. Energy Storage* **2019**, *26*, 101034.
[16] Y. Sheng, C. R. Fell, Y. K. Son, B. M. Metz, J. Jiang, B. C. Church, *Front. Energy Res.* **2014**, *2*, 56.
[17] A. Ngandjong, T. Lombardo, E. Primo, M. Chouchane, A. Shodiev, O. Arcelus, A. A. Franco, *J. Power Sources* **2021**, *485*, 229320.
[18] O. Schmidt, M. Thomitzek, F. Röder, S. Thiede, C. Herrmann, U. Krewer, *J. Electrochem. Soc.* **2020**, *167*, 060501.
[19] G. Lenze, F. Röder, H. Bockholt, W. Haselrieder, A. Kwade, U. Krewer, *J. Electrochem. Soc.* **2017**, *164*, A1223.
[20] C. Meyer, M. Kosfeld, W. Haselrieder, A. Kwade, *J. Energy Storage* **2018**, *18*, 371.
[21] C. Meyer, H. Bockholt, W. Haselrieder, A. Kwade, *J. Mater. Process. Technol.* **2017**, *249*, 172.
[22] C. Schilcher, C. Meyer, A. Kwade, *Energy Technol.* **2016**, *4*, 1604.
[23] C. Meyer, M. Weyhe, W. Haselrieder, A. Kwade, *Energy Technol.* **2020**, *8*, 1900175.
[24] E. N. Primo, M. Chouchane, M. Touzin, P. Vazquez, A. A. Franco, *J. Power Sources* **2021**, *488*, 229361.
[25] M. M. Loghavi, S. Bahadorikhalili, N. Lari, M. H. Moghim, M. Babaiee, R. Eqra, *Zeitschrift fur Phys. Chemie* **2020**, *234*, 381.
[26] M. Haarmann, W. Haselrieder, A. Kwade, *Energy Technol.* **2020**, *8*, 1801169.
[27] M. Park, X. Zhang, M. Chung, G. B. Less, A. M. Sastry, *J. Power Sources* **2010**, *195*, 7904.
[28] V. J. Ovejas, A. Cuadras, *J. Power Sources* **2019**, *418*, 176.

[29] R. Tian, S.-H. Park, P. J. King, G. Cunningham, J. Coelho, V. Nicolosi, J. N. Coleman, *Nat. Commun.* **2019**, *10*, 1933.
[30] L. S. de Vasconcelos, N. Sharma, R. Xu, K. Zhao, *Exp. Mech.* **2019**, *59*, 337.
[31] H. Kondo, H. Sawada, C. Okuda, T. Sasaki, *J. Electrochem. Soc.* **2019**, *166*, A1285.
[32] N. Billot, T. Günther, D. Schreiner, R. Stahl, J. Kranner, M. Beyer, G. Reinhart, *Energy Technol.* **2020**, *8*, 1801136.
[33] D. Schreiner, M. Oguntke, T. Günther, G. Reinhart, *Energy Technol.* **2019**, *7*, 1900840.
[34] D. Shin, M. Poncino, E. Macii, N. Chang, In *International Symposium on Low Power Electronics and Design (ISLPED)*; 2013; pp. 94–99.
[35] W. Yourey, *Batteries* **2020**, *6*, 23.
[36] B. Suthar, P. W. C. Northrop, D. Rife, V. R. Subramanian, *J. Electrochem. Soc.* **2015**, *162*, A1708.
[37] R. W. Heckel, *Trans. Metall. Soc. AIME* **1961**, *221*, 671.
[38] W. C. Oliver, G. M. Pharr, *J. Mater. Res.* **1992**, *7*, 1564.
[39] A. Rucci, A. C. Ngandjong, E. N. Primo, M. Maiza, A. A. Franco, *Electrochim. Acta* **2019**, *312*, 168.

Manuscript received: December 17, 2020
Revised manuscript received: February 4, 2021
Accepted manuscript online: February 18, 2021
Version of record online: March 1, 2021

